Ultrasonic investigation of field-dependent ordered phases in the filled skutterudite compound $PrOs_4As_{12}$

T. Yanagisawa, W. M. Yuhasz,* T. A. Sayles, P.-C. Ho,† and M. B. Maple
Department of Physics and Institute for Pure and Applied Physical Sciences, University of California San Diego, La Jolla, California 92093, USA

H. Watanabe, Y. Yasumoto, Y. Nemoto, and T. Goto
Graduate School of Science and Technology, Niigata University, Niigata 950-2181, Japan

Z. Henkie and A. Pietraszko
Institute for Low Temperature and Structural Research, Polish Academy of Science, 50-950 Wrocław, Poland
(Received 5 April 2007; revised manuscript received 13 January 2008; published 28 March 2008)

Elastic constant measurements down to 0.48 K and in magnetic fields up to 11 T were performed on a single crystal of the filled skutterudite compound $PrOs_4As_{12}$. The longitudinal $C_{L111}=C_B+4C_{44}/3$ mode shows Curie-type softening below ~25 K, which is explained in terms of the quadrupole susceptibility modified by a crystalline electric field with a $\Gamma_4^{(2)}$ ground state. A detailed *H-T* phase diagram for $H\|[111]$ is compiled with the elastic anomalies, which appear on the boundaries of two ordered phases at temperatures below 2.3 K and in fields below 3 T. The intermediate phase between 2 and 2.5 T assumes the aspect of antiferroquadrupolar ordering.

DOI: 10.1103/PhysRevB.77.094435 PACS number(s): 71.20.Eh, 71.27.+a, 62.20.D−, 71.70.Ch

I. INTRODUCTION

The filled skutterudite compounds with the formula AT_4X_{12} (A=alkali metal, alkaline earth, lanthanide, or actinide; T=Fe, Ru, or Os; X=P, As, or Sb) display a variety of strongly correlated electron phenomena due to the strong hybridization between lanthanide-filler-ion-localized $4f$ states and conduction electron states. In addition, local atomic vibrations of the lanthanide filler ion in an anharmonic potential of an oversized cage consisting of T and X atoms, so-called rattling, cause a significant reduction of thermal conductivity in these compounds.[1] The filled skutterudites are expected to be a candidate system for exotic local phonon problems related to the multichannel Kondo effect, the theory of which has recently been extensively studied.[2,3] The ultrasonic wave associated with the elastic strain is generally useful for observing the electric quadrupole moment due to the charge distribution that results from the off-center motion of ions as well as the orbital degrees of freedom in $3d$- and $4f$-electron systems.[4,5] Ultrasonic studies of the filled skutterudites have achieved intriguing results, such as the determination of a Γ_{23} off-center mode in the heavy fermion superconductor $PrOs_4Sb_{12}$ and indications of quadrupole ordering in $PrFe_4P_{12}$.[6,7] The characterization of the filled skutterudite arsenides has progressed recently, with the successful synthesis of filled skutterudite arsenide single crystals.

Specific heat measurements of $PrOs_4As_{12}$ display a sharp peak at $T_1 \sim 2.2$ K and a broad maximum at $T_2 \sim 2.3$ K.[8] In zero magnetic field, the low-temperature phase has been identified as antiferromagnetic (AFM) ordering by neutron scattering.[9] Until neutron scattering measurements are performed in a magnetic field, the nature of a second ordered phase between 1.5 and 3 T remains unclear. Along with observed magnetic ordering, measurements of the specific heat of $PrOs_4As_{12}$ indicate heavy fermion behavior. Fits to the magnetic susceptibility based on an estimate of the magnetic moment at low temperatures indicate that the Pr^{3+} ion could have a magnetic Γ_5 triplet ground state with either a nonmagnetic Γ_1 or Γ_3 first excited state analyzed by assuming cubic O_h symmetry. In the present paper, we report on the results of elastic property measurements performed on $PrOs_4As_{12}$ single crystals. Since the magnetic Γ_5 triplet ground state in $PrOs_4As_{12}$ possesses all the electric quadrupole moments O_2^0, O_2^2, O_{yz}, O_{zx}, and O_{xy} in O_h symmetry, which favor quadrupolar ordering, as well as magnetic dipoles, it is important to measure the elastic constant in terms of the quadrupole susceptibility to extract the crystalline electric field (CEF) level scheme and possible coexistence of quadrupole ordering in the ordered phase much like the typical antiferroquadrupolar (AFQ) ordered compound CeB_6.[10]

II. EXPERIMENTAL DETAILS

Single crystals of $PrOs_4As_{12}$ were grown by means of a metallic flux growth method at high pressure as described in Ref. 9. The unit cell of $PrOs_4As_{12}$ has the $LaFe_4P_{12}$-type bcc structure with space group $T_h^5(Im\bar{3})$ and a lattice constant a =8.5319(11) Å. A small octahedron-shaped specimen with facets that are perpendicular to the [111] direction was used for the ultrasonic measurement. The sound was generated and detected by piezoelectric $LiNbO_3$ transducers bonded to the parallel [111] facets with a distance of ~0.69 mm between them. The relative change of sound velocity $\Delta v/v$ was detected by a phase comparator using a double balanced mixer. In the present measurements, the absolute value of the sound velocity v_{ij} could not be estimated because the sample thickness was not enough. A ^{3}He evaporation refrigerator and a superconducting magnet were used for measurements

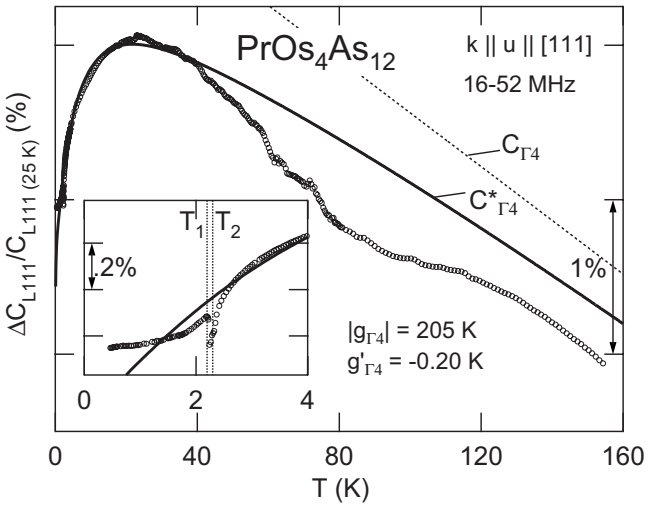

FIG. 1. Relative change of elastic constant C_{L111} as a function of temperature at frequencies of 16 MHz ($80 \leq T \leq 150$ K) and 52 MHz ($0.5 \leq T \leq 80$ K), with a CEF fit for $PrOs_4As_{12}$. The inset displays an enlarged view below 4 K. The two transitions at $T_1 \sim 2.2$ K and $T_2 \sim 2.3$ K are indicated by the vertical dotted lines. The solid line is the calculated quadrupole susceptibility with the parameters $W=4.8009$, $x=0.5292$, $y=0.02$, $|g_{\Gamma 4}|=205$ K, and $g'_{\Gamma 4}=-0.20$ K (symbols are defined in text). The dashed line is the background of the unperturbed mode $C^{*0}_{\Gamma 4}=C_B+(4/3)C^0_{\Gamma 4}=C_B+(4/3)(2.565-0.004T)\times 10^{10}$ J/m^3.

down to 0.48 K in fields up to 11 T. The elastic constant C_{L111} was obtained by using longitudinal ultrasonic waves that propagate along the [111] axis with frequencies from 16 to 52 MHz.

III. RESULTS AND DISCUSSION

A. Quadrupolar susceptibility

Figure 1 displays the relative change of longitudinal elastic constant C_{L111} as a function of temperature, and the solid line is a theoretical fit. The data in Fig. 1 consist of two measurements performed at frequencies of 16 and 52 MHz, in temperature ranges of $80 \leq T \leq 150$ K and $0.5 \leq T \leq 80$ K, respectively. Softening proportional to the reciprocal temperature with a size of 1% is observed from 25 down to ~2.5 K. The C_{L111} elastic constant under zero magnetic field can be rewritten as $C_{L111}=C_B+4C_{44}/3$ in T_h symmetry, where $C_B=(C_{11}+2C_{12})/3$ is the bulk modulus, corresponding to the total symmetric volume strain ε_B associated with Γ_1 symmetry. The transverse C_{44} mode consists of the symmetry-breaking strain ε_{yz}, ε_{zx}, and ε_{xy} associated with $\Gamma_4^{(2)}$ symmetry. Since the absolute value of the sound velocity could not be estimated in the present measurement, we use the absolute values of the elastic constants $C_B=27.64\times 10^{10}$ J/m^3 and $C_{44}=2.274\times 10^{10}$ J/m^3 at 25 K observed in $PrOs_4Sb_{12}$,[11,12] as a substitute for calculation of the elastic constant C_{L111} in $PrOs_4As_{12}$. In the present case, we also assume that the softening of C_{L111} between 25 and 4 K is dominated by the C_{44} mode and is affected by the CEF with a $\Gamma_4^{(2)}$ triplet ground state. The C_{L111} below 4 K (Fig. 1, inset) reveals enhanced softening at $T_2 \sim 2.3$ K followed by a rapid increase in C_{L111} at $T_1 \sim 2.2$ K, where T_2 denotes the transition temperature from paramagnetic phase I to intermediate phase II, and T_1 denotes the transition temperature from phase II to AFM phase III (see Fig. 4), which are consistent with the previous specific heat measurements.[8,9] In phase III, below T_1, C_{L111} decreases slowly down to 0.5 K and slowly levels off at the lowest temperatures. In the temperature range $40 \leq T \leq 120$ K, C_{L111} deviates from the theoretical fit $C_{\Gamma 4}$, and shows a broad upturn. The deviation seems to be an ultrasonic dispersion due to rattling, which also appears in the Γ_{23}-related elastic constants of $PrOs_4Sb_{12}$ and $NdOs_4Sb_{12}$.[6,13] However, unlike these compounds, neither frequency dependence nor deterioration of the ultrasonic echoes is detected in the C_{L111} mode of $PrOs_4As_{12}$. Since only the Γ_{23} symmetry off-center mode couples to Γ_{23}-related strain waves, such as the $(C_{11}-C_{12})/2$ mode, C_{11}, and C_{L110} elastic constants in the cubic system, the C_{44} dominant mode measured in $PrOs_4As_{12}$, which is related to Γ_4 symmetry strains and couples to the Γ_4 off-center mode, is less likely to show ultrasonic dispersion. Recent measurements by Nakanishi *et al.* indicate a distinct upturn in the C_{44} mode of $PrOs_4Sb_{12}$,[14] which disagrees with the above scenario; therefore, to clarify these issues, the Γ_{23}-related elastic constants need to be measured in $PrOs_4As_{12}$.

The ninefold-degenerate $J=4$ Hund's rule ground state multiplet of the Pr^{3+} ion splits into a Γ_1 singlet, a Γ_{23} doublet, and $\Gamma_4^{(1)}$ and $\Gamma_4^{(2)}$ triplet states in a tetrahedral T_h CEF. See Ref. 29 for the definition of the triplet state wave functions in T_h symmetry. The elastic softening of the C_{L111} mode can be described in terms of the quadrupole susceptibility of the quadrupole moments O_{xy}, O_{yz}, and O_{zx} with $\Gamma_4^{(2)}$ symmetry in a CEF energy level scheme with a $\Gamma_4^{(2)}$ triplet ground state.

The solid line in Fig. 1 shows a modified quadrupole susceptibility $C^*_{\Gamma 4}=C_B+4C_{\Gamma 4}/3$ for best fit to the elastic constant C_{L111}. (see the Appendix for detailed fomulation of the quadrupole susceptibility) Here, the bulk modulus C_B is assumed to be constant at low temperatures as $C_B=27.64\times 10^{10}$ J/m^3, which is the value for $PrOs_4Sb_{12}$ at 25 K.[11,12] The background C^0_{L111} (dashed line) is extrapolated from the slope of the high-temperature data shown in Fig. 1. By considering information about the CEF ground state from recently performed inelastic neutron scattering results, which include peak positions at 0.4, 13, and 23 meV for $PrOs_4As_{12}$,[15] the CEF parameters for the best fit were inferred from the fit as follows: $W=4.8189$, $x=0.5330$, and $y=0.02$ with CEF energy level scheme $\Gamma_4^{(2)}$(0 K)-Γ_1(4.6 K)-Γ_{23}(158.6 K)-$\Gamma_4^{(1)}$(267.0 K). The parameter x represents the ratio between the fourth- and sixth-degree terms for cubic symmetry and W represents an energy scaling factor of the CEF Hamiltonian. The additional tetrahedral term parameter y was assumed to have a nonzero value. The parameter $y=0.02$ was found for $PrOs_4As_{12}$, which is smaller than the value of $y=0.105$ previously determined for $PrOs_4Sb_{12}$ by Kohgi *et al.*[16] The coupling constants $|g_{\Gamma 4}|=205$ K and $g'_{\Gamma 4}=-0.20$ K are obtained for $PrOs_4As_{12}$. The value of $g'_{\Gamma 4}$ is negative, which suggests that the intersite interactions of the $\Gamma_4^{(2)}$ quadrupoles in $PrOs_4As_{12}$ are of

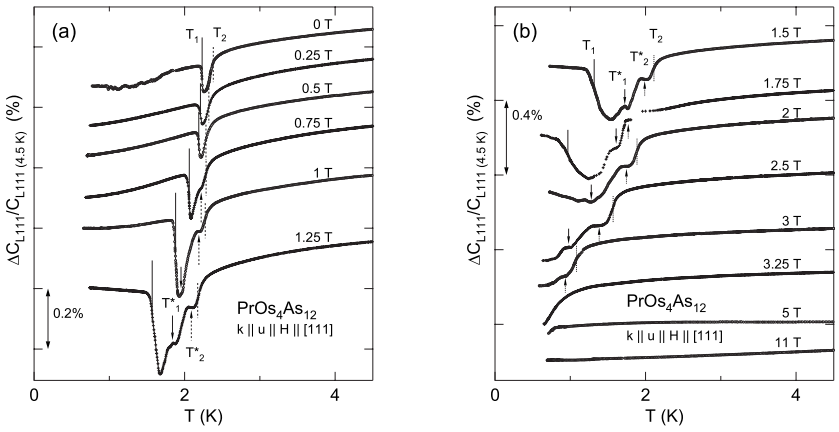

FIG. 2. Relative change of the elastic constant $\Delta C_{L111}/C_{L111}$ vs temperature at several fixed magnetic fields along the [111] axis of a $PrOs_4As_{12}$ single crystal, for (a) $0 \leq H \leq 1.25$ T and (b) $1.5 \leq H \leq 11$ T. Arrows indicate the observed elastic anomalies (see text).

antiferro-quadrupolar type, much like the value of −0.07 K found for $PrOs_4Sb_{12}$.[11] The previously reported magnetic susceptibility analysis in O_h symmetry[9] found that the energy gap between the Γ_5 ground state and the Γ_1 first excited state has a much larger value $\Delta \sim 17$ K than the currently used value $\Delta \sim 4.6$ K. Since both CEF parameters can reproduce the Curie-type softening with small change of coupling constants, at least in the present analysis of the elastic constant, we can conclude that $PrOs_4As_{12}$ has the Γ_5-Γ_1 pseudoquartet ground state with energy gap $\Delta \leq 17$ K.

B. Magnetic field dependence

To investigate the elastic properties in the ordered phase, the magnetic field dependence of C_{L111} has been measured at a frequency of 52 MHz. Figure 2 shows the relative change of the elastic constant $\Delta C_{L111}/C_{L111}$ vs temperature at several fixed magnetic fields parallel to the [111] axis for $0 \leq H \leq 1.25$ T [Fig. 2(a)] and $1.25 \leq H \leq 11$ T [Fig. 2(b)]. In low fields ($0 \leq H \leq 0.75$ T), as T decreases, $\Delta C_{L111}/C_{L111}$ shows a sudden decrease at T_2 and a steplike increase at T_1, which mark the boundaries of a narrow intermediate region identified as phase II in the H-T phase diagram (see Fig. 4). Here, the transition temperature T_1 is defined as the minimum and T_2 is the maximum in the first derivative. As the magnetic field is increased, the lower transition T_1, which is indicated by vertical solid lines, shifts to lower temperatures and the depth of the minimum between T_1 and T_2 gradually increases. At fields above 0.75 T and temperatures below T_2, a plateau was detected at T_2^*, which also shifts to lower temperatures with increasing fields as indicated by the upper arrows. In higher fields above 1 T, another plateau, indicated by the lower arrows in Fig. 2, appears between the minimum and the upper plateau of $\Delta C_{L111}/C_{L111}$ at T_1^*. The minimum in $\Delta C_{L111}/C_{L111}$ gets broader for fields between 1.5 and 2 T and eventually T_1 is suppressed by 2 T. In the field range $3 \leq H \leq 5$ T, only a precursory change of T_2 was detected, and C_{L111} exhibits a monotonic decrease with decreasing temperature for $H \geq 5$ T. In general, T_2 and T_2^* are less sensitive to increasing magnetic field than T_1. The sudden softening in the ultrasonic data of $PrOs_4As_{12}$ in a very narrow region below T_2 (Fig. 2) is reminiscent of typical quadrupole ordering compounds such as CeB_6 and $Ce_xLa_{1-x}B_6$,[17–19] which have a cubic structure, as well as DyB_2C_2 and HoB_2C_2,[20] which have a tetragonal structure. These compounds have an AFQ and AFM coexisting phase as the ground state. In addition, an unknown intermediate ordered phase exists, the so-called phase IV for $Ce_xLa_{1-x}B_6$ with $0.65 \leq x \leq 0.75$ and HoB_2C_2.[21–24] The transverse C_{44} in $Ce_xLa_{1-x}B_6$ ($0.65 \leq x \leq 0.75$) shows huge softening of a size 20%–30% with strong ultrasonic attenuation in phase IV.

Recent theoretical studies proposed that the order parameter of phase IV for $Ce_xLa_{1-x}B_6$ is considered to be Γ_5-type octupoles which induce Γ_5 quadrupole moments even in zero field.[25]

In $PrOs_4As_{12}$, we noticed that the ultrasonic echoes deteriorate in the intermediate phase II, suggesting that quadrupole fluctuations occur in a narrow temperature range for $T_1^* \leq T \leq T_2$ (Fig. 2). Quadrupole fluctuations have also been observed in phase IV of $Ce_xLa_{1-x}B_6$. The change in the elastic constant $\Delta C_{44}/C_{44}$ observed in phase IV of $Ce_xLa_{1-x}B_6$ is ~20% due to the induced ferroquadrupole moment, while the change in $\Delta C_{L111}/C_{L111}$ of $PrOs_4As_{12}$ is much smaller (~0.4%) in phase II (at 2.5 T).

Figure 3 shows the magnetic field dependence of the relative change in the elastic constant $\Delta C_{L111}/C_{L111}$ at several fixed temperatures from 485 mK to 3 K in magnetic fields up to 11 T applied along the [111] axis. The elastic constant C_{L111} displays a broad minimum around 1 T, with successive transitions between 2 and 3 T. The vertical lines and arrows in Fig. 3 indicate elastic anomalies that are consistent with four anomalies displayed in Fig. 2; a steplike anomaly at H_1 and H_2 (solid and dotted lines), a plateau at H_2^*, and an intermediate kink at H_1^* (lower and upper arrows) which are related to T_2^* and T_1^* in Fig. 2, respectively. The region between H_1 and H_1^* becomes narrower and all the anomalies shift to lower fields with increasing temperature. In the paramagnetic state, above H_2 for all fixed temperatures, C_{L111} exhibits a broad maximum around 8 T, which may be due to Zeeman splitting of the CEF energy levels. At temperatures between 2.5 and 3 K, no elastic anomaly was observed. The curvature, in the paramagnetic phase above H_2, deviates slightly from the calculated behavior by using the present CEF model (not shown). The CEF calculations indicate no level crossing for $H \| [111]$ up to 30 T, which suggests that the field-induced ordered phase found in $PrOs_4Sb_{12}$ is less likely to occur in $PrOs_4As_{12}$. Since magnetic anisotropy of the CEF level splitting was also expected from the current

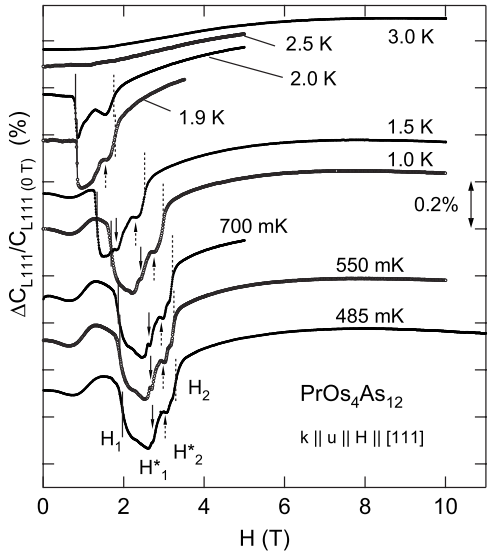

FIG. 3. Relative change of the elastic constant $\Delta C_{L111}/C_{L111}$ vs magnetic field ($H\|[111]$) at several fixed temperatures for a $PrOs_4As_{12}$ single crystal. Vertical solid and dotted lines and arrows indicate the observed elastic anomalies (see text).

CEF model, further measurements in field are needed along other orientations (e.g., $H\|[100]$ and $[110]$).

C. *H-T* phase diagram

Figures 4(a) and 4(b) show the magnetic field–temperature (H-T) phase diagrams for $PrOs_4As_{12}$, determined from the elastic anomalies in C_{L111} vs T (Fig. 2) and C_{L111} vs H (Fig. 3). The circles in the left figure are associated with the rapid increase at T_1 and H_1 and sudden softening at T_2 and H_2, which agree with the transition points previously determined from magnetization measurements.[9] Several points, which were newly observed in the present work, in phase II are plotted separately in Fig. 4(b). In Figs. 4(a) and 4(b), the vertical and horizontal bars represent the transition width, defined by the change of the curvature for transitions T_i and H_i, and the width of the plateau for T_i^* and H_i^* $(i=1,2)$. The open triangles, associated with the lower dip at T_1^* (H_1^*), in Fig. 4(b) outline another phase boundary in the middle of phase II. The solid and open diamonds, in Fig. 4(b), which indicate the minima in C_{L111}, overlap the II-III phase boundary at high temperatures in zero field and eventually merge with the II-II′ phase boundary at T_1^* or H_1^* (open triangles) around 2.5 T. The layout of this phase diagram is similar to the typical AFQ compounds CeB_6 and DyB_2C_2.[26,27] In addition, the $\Delta C_{L111}/C_{L111}$ vs T data in Fig. 2(b) feature a shallow minimum at 2 T below 1 K, which is reminiscent of the elastic constant C_{44} for the AFQ transitions in CeB_6 and the DyB_2C_2.[18,20] The direct product of the Γ_4 triplet is $\Gamma_4 \otimes \Gamma_4 = \Gamma_1 \oplus \Gamma_{23} \oplus 2\Gamma_4$, which has nine degrees of electric and magnetic freedom, implying that the magnetic $\Gamma_4^{(2)}$ triplet ground state has an electric quadrupole moment as well as in the case of a $\Gamma_4^{(2)}$-Γ_1 pseudoquartet. Therefore, the disappearance of softening of C_{L111} in intermediate phase II of $PrOs_4As_{12}$ suggests that the degenerate ground state, which could consist of a $\Gamma_4^{(2)}$ triplet or a $\Gamma_4^{(2)}$-Γ_1 pseudoquartet, is split due to magnetic or quadrupole ordering. We conclude from this that phase II′ for $T \leq 1$ K and $2.0 \leq H \leq 2.5$ T should be distinguished from phase II. The negative intersite quadrupole interaction constant g_Γ' for $PrOs_4As_{12}$ indicates that AFQ ordering may be a candidate for the order parameter in phase II′, between T_1 and the minimum in C_{L111} vs T [Fig. 2(b)]. However, the question of whether phases II and II′ are due to quadrupole ordering or not still remains open. Further experiments, in particular microscopic measurements such as resonant x-ray or neutron scattering, should be performed to clarify the order parameter and the actual ordered structure in phase II.

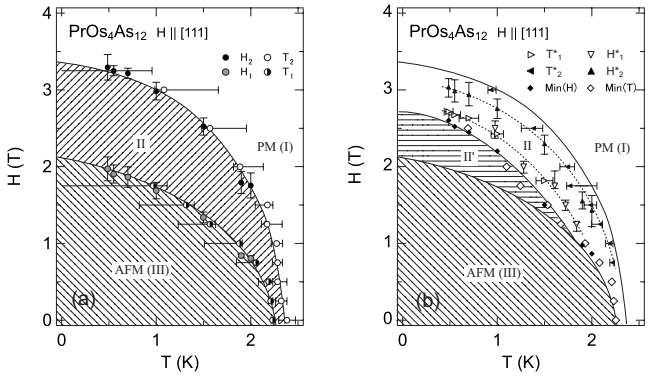

FIG. 4. Magnetic field–temperature (H-T) phase diagrams for $PrOs_4As_{12}$ along the [111] axis, compiled from features in the elastic constant C_{L111}. (a) H_2 and H_1 (solid circles), T_2 and T_1 (open and half-solid circles). (b) Upper dip T_2^* and H_2^* (solid triangles), lower dip T_1^* and H_1^* (open triangles), and minima (open and solid diamonds). The dotted lines and mesh colors are guides to the eye to distinguish the phases: paramagnetic phase I, antiferromagnetic phase III, and unknown ordered phases II and II′.

IV. SUMMARY

In summary, the Curie-type softening of the C_{L111} elastic constant, displayed by the filled skutterudite compound $PrOs_4As_{12}$, indicates that the Pr^{3+} ion has a $\Gamma_4^{(2)}$ triplet ground state with a Γ_1 singlet first excited state, consistent with previous magnetization measurements. Analysis of the quadrupole susceptibility suggests that the intersite quadrupole interaction in this compound is negative, indicating an antiferroquadrupolar-type interaction. The present ultrasonic measurements define a new phase boundary in the middle of the upper ordered phase II, which may be associated with AFQ ordering.

ACKNOWLEDGMENTS

Research at UCSD was supported by the U.S. Department of Energy under Grant No. DE-FG02-04ER46105 and the U.S. National Science Foundation under Grant No. DMR-0335173. Research at Niigata University was supported by a Grant-in-Aid for Scientific Research Priority Area "Skutterudite" of the Ministry of Education, Culture, Sports, Science and Technology, Japan (Grant No. 15072206). One of the

authors (T.Y.) was supported by the Japan Society of Promotional Science.

APPENDIX: FORMULATION OF THE QUADRUPOLE SUSCEPTIBILITY

This appendix gives a brief review of the formulation of quadrupole susceptibility. We start the formulation with the following Hamiltonian:

$$H = H_{\mathrm{CEF}} + H_{\mathrm{QS}} + H_{\mathrm{QQ}}. \tag{A1}$$

Here H_{CEF} is the Lea, Leask, and Wolf (LLW) CEF Hamiltonian[28] with the additional Takegahara tetrahedral term,[29] which can be written as

$$H_{\mathrm{CEF}} = W\left(x\frac{O_4}{F_4} + (1-x)\frac{O_6}{F_6} + y\frac{O_6^t}{F_6^t}\right), \tag{A2}$$

where $O_4 = O_4^0 + 5O_4^4$, $O_6 = O_6^0 - 21O_6^4$, and $O_6^t = O_6^2 - O_6^6$ are the Stevens equivalent operator O_l^m, which is written as an l-degree polynomial of angular momentum J.[30] $F_4 = 60$, $F_6 = 1260$, and $F_6^t = 30$ are the specific parameters for $J = 4$. The second term in Eq. (A1), H_{QS}, is a single-ion quadrupole-strain interaction,

$$H_{\mathrm{QS}} = -\sum_{\Gamma\gamma} g_\Gamma O_{\Gamma\gamma}\varepsilon_{\Gamma\gamma}, \tag{A3}$$

where g_Γ is a coupling constant. $O_{\Gamma\gamma}$ and $\varepsilon_{\Gamma\gamma}$ are quadrupole operators and strains, respectively, which are listed in Table I.

The third term in Eq. (A1), H_{QQ}, is the intersite quadrupole interaction between rare-earth ions treated in the mean-field approximation,

$$H_{\mathrm{QQ}} = -\sum_{\Gamma\gamma} g'_\Gamma \langle O_{\Gamma\gamma}\rangle O_{\Gamma\gamma}, \tag{A4}$$

where g'_Γ is the interionic quadrupole coupling constant. $\langle O_{\Gamma\gamma}\rangle$ denotes the mean field of the quadrupole. The free energy of the $4f$-electronic states in the CEF can be written as

$$F = U - Nk_BT \ln\sum_n \exp[-E_n(\varepsilon_{\Gamma\gamma})/k_BT], \tag{A5}$$

where N is the number of ions in a unit volume. $E_n(\varepsilon_{\Gamma\gamma})$ is a perturbed CEF level as a function of the strain $\varepsilon_{\Gamma\gamma}$. n is a collective index for both multiplets and their degenerate states. For cubic symmetry, the internal energy U in Eq. (A5) gives the elastic energy for the strained system, which is written as

$$U = \frac{1}{2}\sum_{i=1}^{6}\sum_{j=1}^{6} C_{ij}\varepsilon_i\varepsilon_j = \frac{1}{2}C_{11}(\varepsilon_{xx}^2 + \varepsilon_{yy}^2 + \varepsilon_{zz}^2) + C_{12}(\varepsilon_{xx}\varepsilon_{yy} + \varepsilon_{yy}\varepsilon_{zz} + \varepsilon_{zz}\varepsilon_{xx}) + \frac{1}{2}C_{44}(\varepsilon_{yz}^2 + \varepsilon_{zx}^2 + \varepsilon_{xy}^2), \tag{A6}$$

which can be written in terms of the symmetry strains $\varepsilon_B = \varepsilon_{xx} + \varepsilon_{yy} + \varepsilon_{zz}$, $\varepsilon_u = (2\varepsilon_{zz} - \varepsilon_{xx} - \varepsilon_{yy})/\sqrt{3}$, and $\varepsilon_v = \varepsilon_{xx} - \varepsilon_{yy}$ as

$$U = \frac{1}{2}\frac{1}{3}(C_{11} + 2C_{12})\varepsilon_B^2 + \frac{1}{2}\frac{(C_{11} - C_{12})}{2}(\varepsilon_u^2 + \varepsilon_v^2) + \frac{1}{2}C_{44}(\varepsilon_{yz}^2 + \varepsilon_{zx}^2 + \varepsilon_{xy}^2). \tag{A7}$$

The elastic constant is given by the second-order differential of the free energy F with respect to strain $\varepsilon_{\Gamma\gamma}$,

TABLE I. Quadrupole (Multipole) operators and coupled symmetry strains.

Symmetry	Quadrupole (Multipole)	Strain
Γ_1	$O_B^{(2)} = J_x^2 + J_y^2 + J_z^2$, $O_B^{(4)} = O_4^0 + 5O_4^4$	ε_B
Γ_{23}	$O_u = (2J_z^2 - J_x^2 - J_y^2)/\sqrt{3}$	ε_u
Γ_{23}	$O_v = J_x^2 - J_y^2$	ε_v
$\Gamma_4^{(2)}$	$O_{xy} = J_xJ_y + J_yJ_x$	ε_{xy}
$\Gamma_4^{(2)}$	$O_{yz} = J_yJ_z + J_zJ_y$	ε_{yz}
$\Gamma_4^{(2)}$	$O_{zx} = J_zJ_x + J_xJ_z$	ε_{zx}

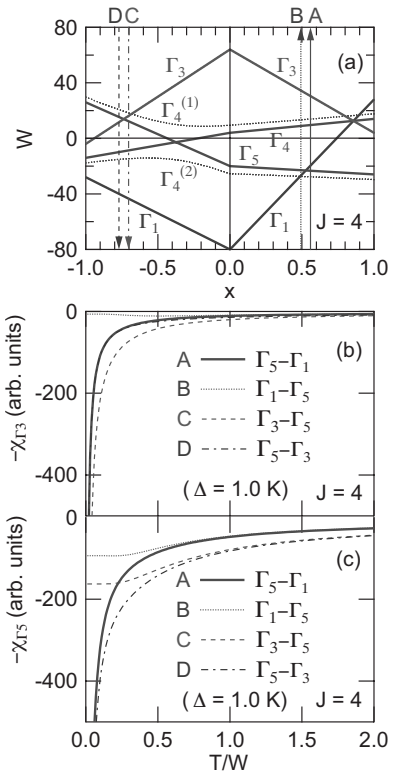

FIG. 5. (a) CEF energy level scheme of Pr^{3+} ($J=4$) for O_h (solid lines) and T_h symmetry (dotted lines). (b) Calculated quadrupole susceptibility $-\chi_{\Gamma3}$ vs scaled temperature W for several CEF ground state models. (c) Calculated quadrupole susceptibility $-\chi_{\Gamma5}$ vs temperature for several CEF ground state models.

$$C_\Gamma(T) = \left(\frac{\partial^2 F}{\partial \varepsilon_{\Gamma\gamma}^2}\right)_{\varepsilon_{\Gamma\gamma}\to 0} = C_\Gamma^0(T) - \frac{N g_\Gamma^2 \chi_\Gamma(T)}{1 - g_\Gamma' \chi_\Gamma(T)}, \quad \text{(A8)}$$

where N indicates the number of rare-earth ions in a unit volume, $O_{\Gamma\gamma}$ is the quadrupole operator, $\varepsilon_{\Gamma\gamma}$ is the symmetrized strain, $\chi_\Gamma(T)$ is the quadrupole susceptibility written as

$$-g_\Gamma^2 \chi_\Gamma(T) = -\frac{1}{k_B T}\left[\left\langle\left(\frac{\partial E_i}{\partial \varepsilon_{\Gamma\gamma}}\right)^2\right\rangle - \left\langle\frac{\partial E_i}{\partial \varepsilon_{\Gamma\gamma}}\right\rangle^2\right] + \left\langle\frac{\partial E_i^2}{\partial \varepsilon_{\Gamma\gamma}^2}\right\rangle, \quad \text{(A9)}$$

and $E_i(\varepsilon_{\Gamma\gamma})$ is the strain dependence of the CEF energy levels in second-order perturbation theory.[31] In the present filled skutterudite case, the ninefold degenerate $^3H_4$ $(J=4)$ ground state of Pr^{3+} splits into Γ_1 (singlet), Γ_{23} (doublet), and $\Gamma_4^{(1)}$ and $\Gamma_4^{(2)}$ (triplets) in the CEF potential of the site with T_h symmetry.

Figure 5(a) shows the variation of the LLW parameter x of the CEF energy level scheme for Pr^{3+} $(J=4)$ in cubic symmetry. A difference between the O_h and T_h symmetries appears only in the $\Gamma_4^{(1)}$ and $\Gamma_4^{(1)}$ triplet levels. The dotted line in Fig. 5(a) shows the corresponding spectra of $\Gamma_4^{(1)}$ and $\Gamma_4^{(2)}$ in T_h symmetry with the Takegahara parameter $y=0.1$ for comparison. The vertical arrows indicate a typical level scheme to show four different combinations of the ground and first excited states: (A) Γ_5-Γ_1, (B) Γ_1-Γ_5, (C) Γ_3-Γ_5, and (D) Γ_5-Γ_3 with energy gap $\Delta=1.0$ K. Figures 5(b) and 5(c) show the temperature dependence of the susceptibilities of Γ_3- and Γ_5-symmetry quadrupoles, respectively, which are calculated using the four ground state models indicated above. Here, the calculations were done using O_h symmetry for simplification. In the present paper, the elastic constant C_{L111} is described by the dominant C_{44} mode, which can be calculated using $-\chi_{\Gamma 5}$ in Eq. (A8). Due to the selection rule, a Curie-type softening (decreasing of the quadrupole susceptibility proportional to the reciprocal temperature) of $-\chi_{\Gamma 5}$ appears only in the case of the Γ_5 triplet ground state.

*Present address: Ames Laboratory, Iowa State University, Ames, Iowa.

†Present address: California State University, Fresno, California.

[1] V. Keppens, D. Mandrus, B. C. Sales, B. C. Chakoumakos, P. Dai, R. Coldea, M. B. Maple, D. A. Gajewski, E. J. Freeman, and S. Bennington, Nature (London) **395**, 876 (1998).

[2] D. L. Cox, Phys. Rev. Lett. **59**, 1240 (1987); D. L. Cox and A. Zawadowski, Adv. Phys. **47**, 599 (1998).

[3] K. Mitsumoto and Y. Ōno, Physica C **426**, 330 (2005); S. Yotsuhashi, M. Kojima, H. Kusunose, and K. Miyake, J. Phys. Soc. Jpn. **74**, 49 (2005); K. Hattori, Y. Hirayama, and K. Miyake, *ibid.* **74**, 3306 (2005).

[4] B. Lüthi, *Physical Acoustics in the Solid*, Springer Series in Solid State Sciences Vol. 148 (Springer, Berlin, 2004).

[5] T. Goto, Y. Nemoto, T. Yamaguchi, T. Yanagisawa, T. Ueno, T. Watanabe, N. Takeda, O. Suzuki, H. Kitazawa, H. Sugawara, and H. Sato, Physica B **383**, 115 (2006).

[6] T. Goto, Y. Nemoto, K. Sakai, T. Yamaguchi, M. Akatsu, T. Yanagisawa, H. Hazama, K. Onuki, H. Sugawara and H. Sato, Phys. Rev. B **69**, 180511(R) (2004).

[7] Y. Nakanishi, T. Simizu, M. Yoshizawa, T. Matsuda, H. Sugawara, and H. Sato, Phys. Rev. B **63**, 184429 (2001).

[8] W. M. Yuhasz, N. P. Butch, T. A. Sayles, P.-C. Ho, J. R. Jeffries, T. Yanagisawa, N. A. Frederick, M. B. Maple, Z. Henkie, A. Pietraszko, S. K. McCall, M. W. McElfresh, and M. J. Fluss, Phys. Rev. B **73**, 144409 (2006).

[9] M. B. Maple, N. P. Butch, N. A. Frederick, P.-C. Ho, J. R. Jeffries, T. A. Sayles, T. Yanagisawa, W. M. Yuhasz, S. Chi, H. J. Kang, J. W. Lynn, Pencheng Dai, S. K. McCall, M. W. McElfresh, M. J. Fluss, Z. Henkie, and A. Pietraszko, Proc. Natl. Acad. Sci. U.S.A. **103**, 6783 (2006).

[10] J. M. Effantin, J. Rossat-Mignot, P. Burlet, H. Bartholin, S. Kunii,and T. Kasuya, J. Magn. Magn. Mater. **47&48**, 145 (1985).

[11] T. Goto, Y. Nemoto, K. Onuki, K. Sakai, T. Yamaguchi, M. Akatsu, T. Yanagisawa, H. Sugawara, and H. Sato, J. Phys. Soc. Jpn. **74**, 263 (2005).

[12] Y. Nemoto, T. Ueno, N. Takeda, T. Yamaguchi, T. Yanagisawa, T. Goto, H. Sugawara, and H. Sato, Physica B **378-380**, 184 (2006).

[13] T. Yanagisawa, W. M. Yuhasz, P.-C. Ho, M. B. Maple, H. Watanabe, T. Ueno, Y. Nemoto, and T. Goto, J. Magn. Magn. Mater. **310**, 223 (2007).

[14] Y. Nakanishi, M. Oikawa, T. Kumagami, H. Sugawara, H. Sato, and M. Yoshizawa, Physica B **359-361**, 910 (2005).

[15] S. Chi, P. Dai, T. Barnes, H. J. Kang, J. W. Lynn, R. Bewley, F. Ye, M. B. Maple, Z. Henkie, and A. Pietraszko (unpublished).

[16] M. Kohgi, K. Iwasa, M. Nakajima, N. Metoki, S. Araki, N. Bernhoeft, J. M. Mignot, A. Gukasov, H. Sato, Y. Aoki, and H. Sugawara, J. Phys. Soc. Jpn. **72**, 1002 (2003).

[17] T. Fujita, M. Suzuki, T. Komatsubara, S. Kunii, T. Kasuya, and T. Ohtsuka, Solid State Commun. **35**, 569 (1980).

[18] O. Suzuki, S. Nakamura, M. Akatsu, Y. Nemoto, T. Goto, and S. Kunii, J. Phys. Soc. Jpn. **74**, 735 (2005).

[19] D. Mannix, Y. Tanaka, D. Carbone, N. Bernhoeft, and S. Kunii, Phys. Rev. Lett. **95**, 117206 (2005).

[20] U. Staub, A. M. Mulders, O. Zaharko, S. Janssen, T. Nakamura, and S. W. Lovesey, Phys. Rev. Lett. **94**, 036408 (2005).

[21] T. Yanagisawa, T. Goto, Y. Nemoto, S. Miyata, R. Watanuki, and K. Suzuki, Phys. Rev. B **67**, 115129 (2003).

[22] O. Suzuki, T. Goto, S. Nakamura, T. Matsumura, and S. Kunii, J. Phys. Soc. Jpn. **67**, 4243 (1998).

[23] T. Tayama, T. Sakakibara, K. Tenya, H. Amitsuka, and S. Kunii, J. Phys. Soc. Jpn. **66**, 2268 (1997).

[24] M. Hiroi, M. Sera, N. Kobayashi, and S. Kunii, Phys. Rev. B **55**, 8339 (1997).

[25] K. Kubo and Y. Kuramoto, J. Phys. Soc. Jpn. **73**, 216 (2004).

[26] S. Nakamura, T. Goto, O. Suzuki, S. Kunii, and S. Sakatsume, Phys. Rev. B **61**, 15203 (2000).

[27] H. Yamauchi, H. Onodera, K. Ohoyama, T. Onimaru, M. Kosaka, M. Ohashi, and Y. Yamaguchi, J. Phys. Soc. Jpn. **68**, 2057 (1999).

[28] K. R. Lea, M. J. M. Leask, and W. P. Wolf, J. Phys. Chem. Solids

23, 1381 (1962).
[29] K. Takegahara, H. Harima, and A. Yanase, J. Phys. Soc. Jpn. **70**, 1190 (2001).
[30] M. T. Hutchings, in *Solid State Physics*, edited by F. Seitz and D. Turnbull (Academic Press, New York, 1964), Vol. 16, p. 227.
[31] P. Thalmeier and B. Lüthi, in *Handbook on the Physics and Chemistry of Rare Earths*, edited by K. A. Gshchneider, Jr. and L. Eyring (North-Holland, Amsterdam, 1991), Vol. 14, p. 311.